Materials Science in Semiconductor Processing ∎ (∎∎∎∎) ∎∎∎–∎∎∎

Contents lists available at ScienceDirect

Materials Science in Semiconductor Processing

journal homepage: www.elsevier.com/locate/mssp

# A comparative electric and dielectric properties of Al/p-Si structures with undoped and Co-doped interfacial PVA layer

A. Kaya [a,*], İ. Yücedağ [b], H. Tecimer [c], S. Altındal [c]

[a] Department of Opticianry, Vocationel School of Medical Sciences, Turgut Ozal University, Ankara, Turkey
[b] Department of Computer Engineering, Technology Faculty, Duzce University, Duzce, Turkey
[c] Department of Physics, Faculty of Science, Gazi University, Ankara, Turkey

ARTICLE INFO

*Keywords:*
Comparing Al/PVA/p-Si and Al/Co-PVA/p-Si structures
Electric and dielectric properties
Voltage dependent
Electric modulus
Ac conductivity

ABSTRACT

In this study, Al/p-Si structures with undoped and Co-doped PVA interfacial layer called $S_1$ and $S_2$ were fabricated and their both electrical and dielectric properties were compared by using 300 kHz capacitance–voltage ($C$–$V$) and conductance–voltage ($G/\omega-V$) measurements at room temperature. Experimental results show that both $C$ and $G$ or dielectric constant ($\varepsilon'$), dielectric loss ($\varepsilon''$) values were found as strongly function of applied bias voltage especially at inverse and accumulation bias regions. It was found that the value of $R_s$ considerably decreases with doping Co metal contrary to conductivity especially in the forward bias region. Such behavior can be attributed to the lack of free charges in pure PVA. The imaginary part of dielectric modulus ($M''$) gives two peaks for $S_1$ corresponding to enough reverse and forward biases and passes from a minimum at about zero bias. Also, it is clear that the minimum of the $M''$ for $S_2$ coincides with the maximum of the $M''$ for $S_1$ at zero bias. As a result, Co-doped PVA considerable improved the performance of structure. In addition, loss tangent (tan$\delta$), ac conductivity ($\sigma_{ac}$) and real part of the electric modulus ($M'$) were obtained and compared each other.

© 2014 Elsevier Ltd. All rights reserved.

## 1. Introduction

Polymeric materials have attracted much attention in both academic and industrial research fields as a consequence of their wide applications. Therefore, polymer electronics has attracted considerably interest in the last decades with the discovery of conducting polymers. The substantial attentiveness has given the production and electrical characterization of organic electronic devices such as metal-semiconductor (MS) and metal-polymer-semiconductor (MPS) type Schottky barrier diodes (SBDs) [1–8]. The use of polymers as dielectrics or interfacial layer between metal and semiconductor has attracted attention in science and technology within the last decade [9–15]. Amongst them polyvinyl alcohol (PVA) has excellent film forming, emulsifying, and adhesive properties with low melting point for the fully hydrolyzed and partially hydrolyzed grades. Although it is also a good insulating material with low conductivity, but their conductivity can be increased by doping some metals such as nickel (Ni), and zinc (Zn), cobalt (Co) [16,17]. Therefore, metal doped PVA or other polymer materials can be used as an interfacial layer to reduce inter-diffusion at M/S interface [14,15].

Dielectric measurements such as the real ($\varepsilon'$), and imaginary ($\varepsilon''$) parts of complex dielectric constant and loss tangent (tan$\delta=\varepsilon''/\varepsilon'$) are drastically affected by the presence dopant/dopants metal in the polymer [18,19]. It is well known PVA has a very high dielectric strength ($>1000$ kV/mm), good charge storage capacity, and dopant-dependent electrical and optical properties [20].

* Corresponding author.
*E-mail address:* ahmetkaya0107@hotmail.com (A. Kaya).

http://dx.doi.org/10.1016/j.mssp.2014.03.015
1369-8001/© 2014 Elsevier Ltd. All rights reserved.

ARTICLE IN PRESS



Electrical and dielectric properties of PVA are influenced not only by dopant structure and nature but also by doping concentration and procedure [21,22]. The performance of MS and MPS and similar devices are also considerably influenced by the production processes, the thickness of polymer layer and its homogeneity, surface charges or interface traps/states ($N_{ss}$) localized at M/S interface, series resistance of device ($R_s$). In the real MIS, MPS, and other structures, the localized interface states ($N_{ss}$) exist at semiconductor/insulator interface and the device behavior is different from ideal situation due to existence of the $N_{ss}$ and $R_s$ [13,23].The effect of dipoles at the interface on dielectric properties is also important. Usually, the polarization can be classified in four categories namely: electronic ($\alpha_e$) atomic/ionic ($\alpha_a$), oriental/dipolar ($\alpha_o$) and interfacial ($\alpha_i$) [24–26] and each polarization mechanism involves a short range motion of the charge and contributes to total polarization of the material. Among them electronic polarization may be occurred at very high frequencies ($f>10^{15}$ Hz). Atomic polarization may be occurred between $10^{10}$ and $10^{13}$ Hz. On the other hand, dipolar polarization can occur in intermediate or high frequencies ranges of 1 kHz-1 MHz due to their longer relaxation time and may originate from the existence of permanent orient-able dipoles, impurities and surface charges or this locations [24–26]. The interfacial polarization is more sensitive especially in the low frequencies ($f \leq 1$ kHz) [27]. Our measurements carried out 300 kHz. Therefore, last two types of polarizations may be dominant in our dielectric calculations. Especially, the interfacial polarization occurs when mobile charge carriers are impeded by a physical barrier that inhibits charge migration. Thus, the charges pile up at the barrier producing a localized polarization of the materials [27]. According to Tung [28], at a polycrystalline M/S interface, the bonding geometry likely changes from place to place, leading to a locally varying interface dipole. Therefore, the measured BH then reflects some weighted average of this interface dipole. So the Schottky dipole is assumed to arise from the polarization of interface bonds.

In this study, to comparative both the electrical and dielectric properties and ac electrical conductivity of Al/p-Si structures with undoped and Co-doped interfacial PVA layer called (Sample:$S_1$) and (Sample:$S_2$) were fabricated on the same wafer. The variation of both electrical and dielectric properties of these structures including dielectric constant ($\varepsilon'$), dielectric loss ($\varepsilon''$), loss tangent (tan$\delta$), ac electrical conductivity ($\sigma_{ac}$) and real and imaginary parts of electric modulus ($M'$ and $M''$) have been investigated over the applied bias voltage for 300 kHz at room temperature and compared each other. The experimental $C$–$V$ and $G/\omega-V$ measurements were carried out in the wide range of voltage ($-5$ V to 6 V) by using an HP4192 A impedance analyzer at room temperature.

## 2. Experimental procedures

The Al/p-Si structures with and without Co-doped PVA interfacial layer were produced on p-type (B-doped) single crystal Si wafer with (1 1 1) float zone, 350 μm thickness, 0.04 Ω cm resistivity. First semiconductor wafer was cleaned in a mix of a peroxide-ammoniac solution and also in $H_2O+HCl$ solution in 10 min. Si wafer was well rinsed in de-ionized water with 18 MΩ cm resistivity at ultrasonic bath for 15 min and then high naivety Au (99.999%) with ~2000 Å was thermally evaporated atop the back side of Si at about $10^{-6}$ Torr. To ensure a low resistivity ohmic contact, Si wafer was also annealed at 450 °C for 5 min in dry nitrogen ($N_2$) atmosphere. With undoped and Co-doped thin PVA film were produced on the p-type Si by electro-spinning method. 0.5 g of cobalt acetate was mixed with 1 g of polyvinyl Alcohol (PVA). After vigorous stirring for 2 h at 50 °C, a viscous solution of with and without Co-doped PVA acetates were obtained.

Using a peristaltic syringe pump, the precursor solution was delivered to a metal needle syringe (10 ml) with an inner diameter of 0.9 mm at a constant flow rate of 0.02 ml/h. The needle was connected to a high voltage power supply and positioned in the perpendicular on a clamp. A piece of flat aluminum foil was placed 15 cm below the tip of the needle to collect the nano-fibers. By implementing a high bias voltage (20 kV) on the needle, a fluid jet was ejected from the tip. After electro-spinning process, rectifier contacts with 1 mm in diameter and 1500 Å thick high purity Al was deposited on the PVA surface through a metal shadow mask in high vacuum system at $10^{-6}$ Torr. The value of native $SiO_2$ and Co-doped PVA interfacial layers thickness ($d_i$) were obtained the interfacial layer capacitance at strong accumulation region ($C_i=\varepsilon'\varepsilon_o A/d_i$) as 25.14 Å and 54.5 Å, respectively.

The $C$–$V$ and $G/\omega-V$ measurements were carried out for 300 kHz at room temperature by using a HP 4192 A LF impedance analyzer between $-5$ V and 6 V dc voltages by 50 mV steps. At the same time, a small ac signal 40 $mV_{p-p}$ is applied to the sample in order to meet the requirement. All of these measurements were carried out with the help of a microcomputer through an IEEE-488 AC/DC converter card in the janes-475 cryostat at about $10^{-3}$ Torr to avoid from any external noise or other effects.

## 3. Results and discussions

The forward and reverse-bias $C$ and $G/\omega$ measurements of the Al/p-Si structures with undoped and Co-doped PVA interfacial layer called $S_1$ and $S_2$ were carried out at room temperature and given in Fig. 1(a) and (b), respectively. As can be seen in Fig. 1(a), the $C$–$V$ plot of the $S_2$ for 300 kHz gives two peaks which are corresponding to the inversion and accumulation region. First peak especially can be attributed to a particular density distribution of $D_{it}$ at M/S interface near the energy band gap of Si. The other especially can be attributed to the existence of $R_s$ and interfacial Co-doped PVA layer. At the same time, the $C$–$V$ plot of the $S_1$ for 300 kHz shows that capacitance increases with increasing voltage and gives a peak at depletion region due to the charges at traps [29,30]. On the contrary $C$–$V$ plots, the $G/\omega-V$ plots show nearly a U shape behavior for both of the structures. It is easy to see that the values of the $G/\omega-V$ are $5.85\times10^{-9}$ F for $S_1$ and $6.85\times10^{-8}$ F for $S_2$ at $-5$ V, $3.67\times10^{-10}$ F for $S_1$ and $1.27\times10^{-8}$ F for $S_2$ at zero voltage, and $1.66\times10^{-8}$ F for $S_1$

Please cite this article as: A. Kaya, et al., Materials Science in Semiconductor Processing (2014), http://dx.doi.org/10.1016/j.mssp.2014.03.015

ARTICLE IN PRESS



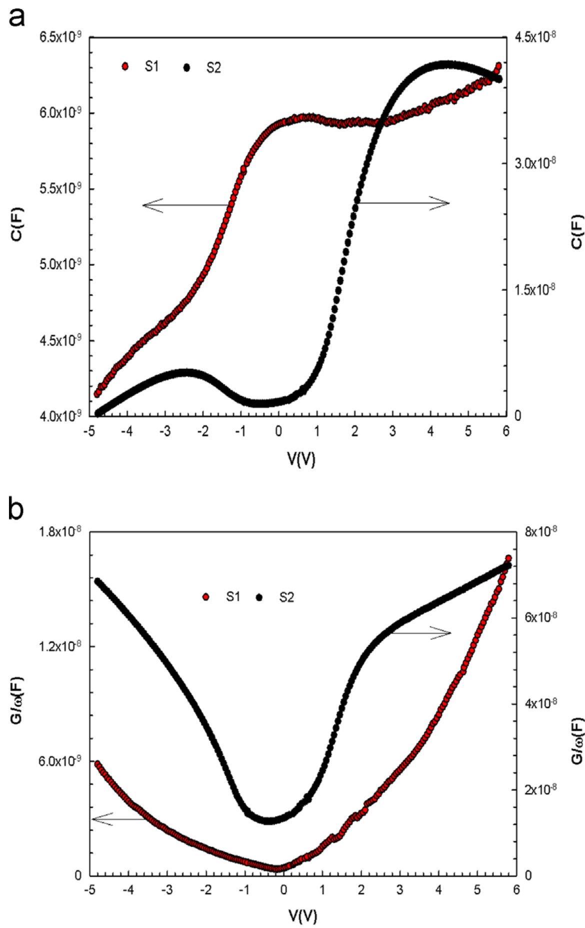


**Fig. 1.** The experimental (a) $C$–$V$ and (b) $G/\omega - V$ plots of the Al/p-Si structures with undoped ($S_1$) and Co-doped ($S_2$) PVA interfacial layer for 300 kHz at room temperature.

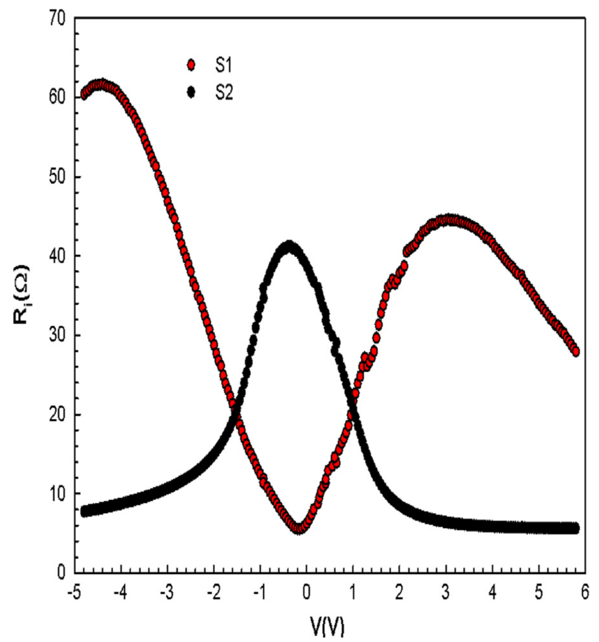


**Fig. 2.** The variation of the resistivity of the Al/p-Si structures with undoped ($S_1$) and Co-doped ($S_2$) PVA interfacial layer as a function bias voltage for 300 kHz at room temperature.

and $7.22 \times 10^{-8}$ F for $S_2$ at +6 V, respectively. It is easy to decide that $S_1$ has higher conductivity than $S_2$.

The value of $R_s$ is effect both electrical and dielectric properties of these devices. For this reason, the voltage dependent of the resistance ($R_i$) of the Al/p-Si structures were obtained by using the $C$ and $G/\omega$ data and admittance method. Using this method and accept that the real value of $R_i$ at enough high frequencies and in strong accumulation region it corresponds to the real value of $R_s$ for that kind of structures and can be computable from the measured $C_{ma}$ and $G_{ma}$ values as following [29],

$$R_s = \frac{G_{ma}}{G_{ma}^2 + \omega^2 C_{ma}^2} \tag{1}$$

where, $\omega$ ($=2\pi f$) is the angular frequency, $C_{ma}$ and $G_{ma}$ are the capacitance and conductance values in the strong accumulation region. The voltage dependent $R_i$ values of $S_1$ and $S_2$ were extracted from Eq. (1) for 300 kHz and are given in Fig. 2. As can be seen in Fig. 2, the $R$–$V$ plots give a distinguishable peak at about zero bias corresponding to the minimum of the $G/\omega - V$ plots for $S_1$. On the contrary $S_1$, $R$–$V$ plots of the $S_2$ shows two peaks like $C$–$V$ plot for at reverse and strong accumulation regions due to particular density distribution of $N_{ss}$ and dopant metal (Co). It may also be restructure and reordering of $N_{ss}$ and other surface charges under applied bias voltage/electric field. As can be clearly seen in Fig. 2, at enough high forward bias regions ($V \geq 6$ V) the real value of resistance corresponds to the $R_s$ of structures. In addition the values of $R_s$ for $S_1$ and $S_2$ samples were found as 27.23 Ω and 5.62 Ω at enough forward bias (6 V) at 300 kHz.

The dielectric constants ($\varepsilon'$ and $\varepsilon''$), loss tangent (tan$\delta$), ac-conductivity ($\sigma_{ac}$), and the real and imaginary parts of electric modulus ($M'$ and $M''$) of the samples were determined using the following expressions [31]:

$$\varepsilon^* = \varepsilon' - j\varepsilon'' = Cd/A\varepsilon_o - j\ (Gd/\omega A\varepsilon_o) \tag{2}$$

$$\tan\ \delta = \varepsilon''/\varepsilon', \tag{3}$$

$$\sigma_{ac} = \omega\varepsilon_0\varepsilon' \tan\ \delta, \tag{4}$$

$$M^* = \frac{1}{\varepsilon^*} = M' + jM'' = \frac{\varepsilon'}{\varepsilon'^2 + \varepsilon''^2} + j\left(\frac{\varepsilon''}{\varepsilon'^2 + \varepsilon''^2}\right) \tag{5}$$

where $\omega$, $d$, $\varepsilon_0$, and $A$ quantities are the angular frequency, the thickness of the PVA, permittivity of the free space ($\varepsilon_0$=8.85 × $10^{-14}$ F/cm), and the rectifier contact area, respectively. Both the obtained dielectric properties and electric modulus values as function of applied bias voltage for frequency of 300 kHz can purvey much information on conductivity contraption and relaxation process for some electronic applications [31,32]. The voltage dependent of $\varepsilon'$, $\varepsilon''$, and tan$\delta$ profiles were obtained using Eqs. 2 and 3, and are given in Fig. 3(a–c), respectively. As can be seen in these figures, the $\varepsilon'$, $\varepsilon''$, and tan$\delta$ values are strongly dependent on applied bias voltage for both of the samples. Our measurements carried out 300 kHz. Therefore, last

Please cite this article as: A. Kaya, et al., Materials Science in Semiconductor Processing (2014), http://dx.doi.org/10.1016/j.mssp.2014.03.015

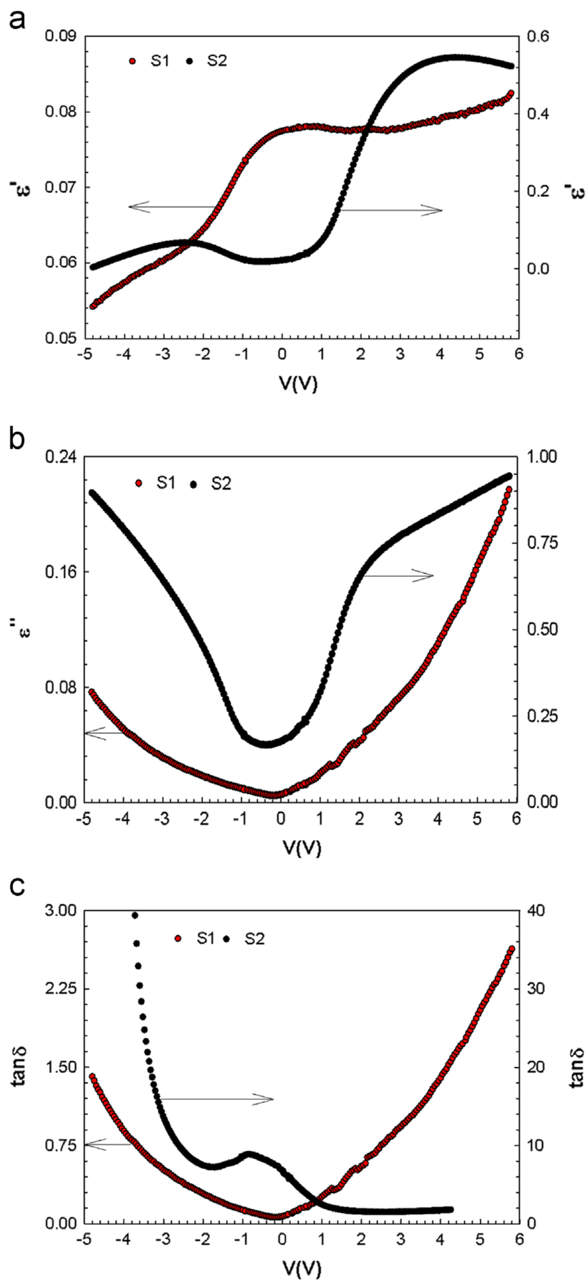


**Fig. 3.** Voltage dependence of the (a) $\varepsilon'$, (b) $\varepsilon''$ and (c) tanδ of the Al/p-Si structures with undoped ($S_1$) and Co-doped ($S_2$) PVA interfacial layer for 300 kHz at room temperature.

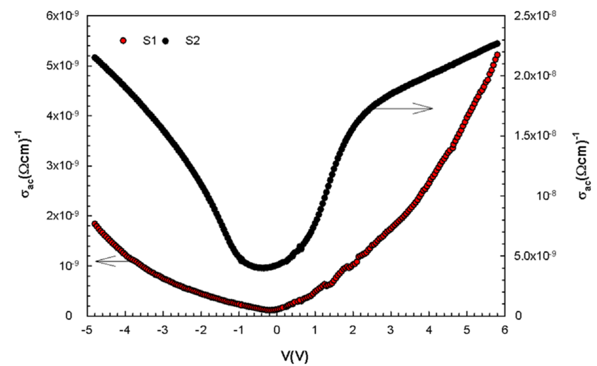


**Fig. 4.** Voltage dependence of the ac electrical conductivity ($\sigma_{ac}$) of the Al/p-Si structures with undoped ($S_1$) and Co-doped ($S_2$) PVA interfacial layer for 300 kHz at room temperature.

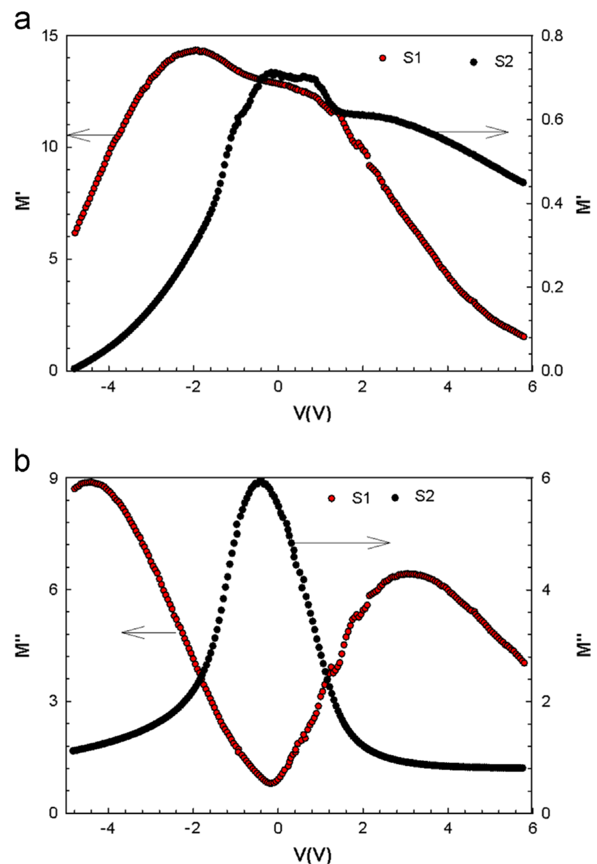


**Fig. 5.** (a) Real part $M'$ and (b) imaginary part $M''$ of electric modulus $M^*$ versus voltage over a measured the Al/p-Si structures with undoped ($S_1$) and Co-doped ($S_2$) PVA interfacial layer for 300 kHz at room temperature.

two type's polarizations (oriental and interfacial) may be dominant in our dielectric calculations.

It is clear to see from these figures, $\varepsilon'$, $\varepsilon''$, and tan$\delta$ vs $V$ profiles were found same as $C$–$V$ and $G/\omega - V$ plots due to same reasons for both of the samples. That kind of behaviors can be ascribed to the interfacial effects within bulk of the samples, interfacial polymer layers, interface traps, surface polarization, and the influences of electrodes [26,32,33].

The $\sigma_{ac}$–$V$ plots were also obtained from the conductivity data and are given in Fig. 4. As shown in this figure the voltage dependent value of $\sigma_{ac}$ increases for $S_2$. The increase in $\sigma_{ac}$ with frequency conductivity accompanied by an increase of the eddy current which in turn increases the tan$\delta$ due to gradual decrease in series resistance [34].

$M'$-$V$ and $M''$-$V$ plots were also obtained by using $\varepsilon'$ and $\varepsilon''$ data for both of the samples and given in Fig. 5(a) and (b), respectively. Plots of the $M'$ show a peak for each samples. The peak of $S_1$ is around -2 V and the other is around zero

bias voltage. In addition, Plot of the $M''$ shows two peaks for $S_1$ and a peak for $S_2$. These properties of $M'$ and $M''$ were attributed to the relaxation polarization in doped polymers and charges at traps. In polymer composite films, the existence of charges at traps gives rise to interfacial polarization. Therefore, it is believed that the dielectric relaxation process in the doped polymer is rather than ones of pure [35]. It is clear that the conductivity of $S_2$ (Co-doped) is higher than the $S_1$, especially at inversion and accumulation regions. In these regions electric field is considerable high according to near zero bias voltage.

## 4. Conclusion

In this study, Al/p-Si structures with undoped and Co-doped PVA interfacial layer which are called $S_1$ and $S_2$ were fabricated on the same wafer and then dielectric parameters such as $\varepsilon'$, $\varepsilon''$, tan$\delta$, $\sigma_{ac}$, $M'$, and $M''$ were obtained by using 300 kHz capacitance–voltage ($C$–$V$) and conductance–voltage ($G/\omega - V$) measurements as function applied bias voltage for 300 kHz at room temperature. In addition, the resistivity of the both samples was obtained as function of applied bias voltage and its effects on dielectric properties were investigated and all properties of the both samples were compared with each other. Experimental results show that both $C$ and $G$ or dielectric constant ($\varepsilon'$), dielectric loss ($\varepsilon''$) values were found as strongly function of applied bias voltage especially at inverse and accumulation bias regions. It was found that the value of $R_s$ considerably decreases with doping Co metal, contrary to conductivity especially in the forward bias region. Such behavior can be attributed to the lack of free charges in pure PVA. In addition, loss tangent (tan$\delta$), ac conductivity ($\sigma_{ac}$) and real part of the electric modulus ($M'$ and $M''$) were obtained and compared each other. The imaginary part of dielectric modulus ($M''$) gives two peaks for $S_1$ which are corresponding to enough reverse and forward biases and passes from a minimum at about zero bias. Also, it is clear that the minimum of the $M''$ for $S_2$ coincides with the maximum of the $M''$ for $S_1$ at zero bias. As a result, Co-doped PVA considerable improved the performance of structure. So, it is clear to see that $S_2$ shows better behavior than $S_1$.

## References

[1] M.E Aydin, F. Yakuphanoglu, J. Eom, D. Hwang, Physica B 387 (2007) 239.
[2] R.K. Gupta, R.A. Singh, Mater. Sci. Semicond. Process. 7 (2004) 83.
[3] S. Rajaputra, G. Sagi, V.P. Singh, Sol. Energy Mater. Sol. Cells 93 (2009) 60.
[4] R.K. Gupta, R.A. Singh, Compos. Sci. Technol. 65 (2005) 677.
[5] Li-Ming Huang, Ten-Chin Wen, A. Gopalan, Thin Solid Films 473 (2005) 300.
[6] P. Syed Abthagir, R. Saraswathi, Org. Electron. 5 (2004) 299.
[7] İ. Yücedağ, A. Kaya, Ş. Altındal, İ. Uslu, Chin. Phys. B 23 (2014) 047304.
[8] A.H. Salama, M Dawy, A.M.A. Nada, Polym. Plast. Technol. Eng 43 (2004) 1067.
[9] S. Altındal, B. Sari, H.I. Unal, N. Yavas, J. Appl. Polym. Sci. 113 (2009) 2955.
[10] J. Zhang, F. Jiang, Chem. Phys. 289 (2003) 243.
[11] N. Dharmaraj, C.H. Kim, H.Y. Kim, Synth. React. Inorg. Met.-Org. Chem. 36 (2006) 29.
[12] G.V. Bazuev, O.I. Gyrdasova, I.G. Grigorov, O.V. Koryakova, Inorg. Mater. 41 (2005) 288.
[13] H. Guan, C. Shao, S. Wen, B. Chen, J. Gong, Xinghua Yang, Mater. Chem. Phys. 82 (2003) 1002.
[14] J.S. Lee, K.H. Choi, H.D. Ghim, S.S. Kim, D.H. Chun, H.Y. Kim, W.S. Lyoo, J. Appl. Polym. Sci 93 (2004) 1638.
[15] H. Saito, B. Stuhn, Polymer 35 (1994) 475.
[16] İ. Dökme, Ş. Altındal, İ. Uslu, J. Appl. Polym. Sci. 125 (2) (2012) 1185.
[17] İ. Dökme, D.E. Yıldız, Ş. Altındal, Adv. Polym. Technol. 31 (2012) 63.
[18] I. Uslu, B. Başer, A. Yaylı, M.L. Aksu, e-Polymers 145 (2007) 1699.
[19] H. Saito, B. Stuhn, Polymer 35 (1994) 475.
[20] Ch.V. Subba Reddy, X. Han, Q.Y. Zhu, L.-Q. Mai, W. Chen, Microelctron. Eng. 83 (2006) 281.
[21] A. Shehap, R.A. Abd Allah, A.F. Basha, F.H. Abdel-Kader, J. Appl. Polym. Sci. 68 (1998) 687.
[22] İ. Dökme, Ş. Altındal, T. Tunc, İ. Uslu, Microelectron. Reliab 50 (2010) 39.
[23] S.M. Sze, Physics of Semiconductor Devices, second ed. Willey & Sons, New York, 1981.
[24] M. Mumtaz, Nawazish A. Khan, Physica C 469 (2009) 182.
[25] A. Kaya, S. Zeyrek, S.E. San, Ş. Altındal, Chin. Phys. B 23 (2014) 018506.
[26] A. Kaya, Ö. Vural, H. Tecimer, S. Demirezen, S. Altındal, Curr. Appl. Phys. 14 (2014) 322–330.
[27] L.L. Hench, J.L. West, Principles of Electronic Ceramics, Wiley, New York, 1990.
[28] R.T. Tung, Phys. Rev. B: Condens. Matter 64 (2001) 205310.
[29] İ. Yücedağ, Optoelectron. Adv. Mater. Rapid Commun. 3 (2009) 612.
[30] P. Cova, A. Singh, R.A. Masut, J. Appl. Phys. 82 (1997) 5217.
[31] N.A. Khan, M. Mumtaz, A.A. Khurram, J. Appl. Phys. 104 (2008) 033916.
[32] İ.M. Afandiyeva, İ. Dökme, Ş. Altındal, M.M. Bülbül, A. Tataroğlu, Microelectron. Eng. 85 (2008) 247.
[33] İ. Yücedağ, Ş. Altındal, A. Tataroğlu, Microelectron. Eng. 84 (2007) 180.
[34] M. Cutroni, A. Mandanici, A. Piccolo, C. Fanggao, G.A. Saunders, P. Mustarelli, Solid State Electron 90 (1996) 167.
[35] N. Bouropoulos, G.C. Psarras, N. Moustakas, A. Chrissanthopoulos, S. Baskoutas, Phys. Status Solidi A 205 (2008) 2033.

Please cite this article as: A. Kaya, et al., Materials Science in Semiconductor Processing (2014), http://dx.doi.org/10.1016/j.mssp.2014.03.015